Many-body effects in multiply charged ion formation in a superstrong laser field

Alexey S. Kornev* and Elena B. Tulenko†
Voronezh State University, 394006 Voronezh, Russia

Boris A. Zon‡
Voronezh State University, 394006 Voronezh, Russia and Belgorod State University, 308015 Belgorod, Russia

We report the numerical calculations for the multiple ionization of rubidium in a strong laser field. We consider multiply charged ion formation and take into account some of the many-body effects, i.e., the inelastic tunneling effect, the collective tunneling, and m relaxation of an ionic core. In the case of strong fields, with intensities in excess of 10^{17} W/cm^2, the free motion of a photoelectron is affected by the magnetic component of the laser field. Because of this, the formation of multiply charged ions as a result of a rescattering process becomes improbable. We present our findings for Rb^{10+} and Rb^{11+} ions, where a significant contribution of collective tunneling was revealed, which was not observed in the weaker fields previously investigated [A. S. Kornev, E. B. Tulenko, and B. A. Zon, Phys. Rev. A **68**, 043414 (2003); Phys. Rev. A **69**, 065401 (2004)].

I. INTRODUCTION

In recent years the formation of multiply charged ions (MCIs) from atoms in the superstrong laser field with an intensity of up to 10^{19} W/cm^2 is under active experimental study (see, e.g., Refs. [1–8]). In fields with such intensities the relativistic effects start to be revealed. The first effect of this kind relates to the influence of the magnetic component of the laser field on a free-electron motion. This effect should be considered as a relativistic one since, as is well known, the Lorentz force is inversely proportional to the speed of light. As a result of the Lorentz force effect, the motion of the electron in the field of the light wave ceases to be a straight line and the electron follows an 8-like trajectory [9]. Therefore, the rescattering processes which dominated in multiple ionization in the fields with lower intensities [10] now become insignificant. The experimental verification of the rescattering suppression due to the relativistic effects was mentioned in Refs. [1,2,4] and carried out in Ref. [5] in the most detailed way.

Since the rescattering process is no longer dominant, multiple ionization occurs due to the direct impact of the laser field on an atom or an ion. The present theory of the tunneling effect [11–14], which is known as the Ammosov-Deloné-Kraĭnov (ADK) theory, as well as its relativistic generalization [15,16], is based on a single-body model. Therefore, multiple ionization in terms of this theory is possible owing to the sequential separation of each electron from a neutral atom or an ion, with a greater multiplicity ion in the ground states formed. Obviously, in this respect, it is desirable to improve the ADK theory by including the many-body effects into consideration.

Previously, the research has been performed by the authors of Refs. [17,18]. Weaker intensities of the laser radiation, which do not lead yet to the relativistic effects, were considered. To avoid the rescattering effects, the laser field under consideration was circularly polarized. The following many-body effects were taken into account: (i) tunneling with ionic core excitation [19], hereinafter called inelastic tunneling effect (ITE); (ii) collective tunneling of several electrons during a single optical half cycle [20] (see also [21]). The results of the calculations for Ne^{2+} ions are in good agreement with the experimental data obtained in Ref. [22]. The results of our theoretical calculations of $Ar^{+}, \ldots, Ar^{6+}$ ion formation probability in Ref. [17] were later examined experimentally in Ref. [23]. In this paper the circularly polarized radiation in the intensity range between 10^{14} and 10^{16} W/cm^2 was used. Experimental data obtained were presented in Ref. [23] for the case of spatially homogeneous laser beam, allowing one to observe the decrease in the yield of n-charged ions, owing to the formation of the ions of greater multiplicity. It should be taken into consideration that such decrease cannot be observed for a beam with a Gaussian distribution of intensity. All experimental data obtained in Ref. [23] agree with the computational results from Ref. [17] very well.

With respect to the role of many-body effects in multiple ionization, the results of Refs. [17,23] confirm the significance of ITE. As for the collective tunneling effect, it does not manifest at the specific range of intensity between 10^{14} and 10^{16} W/cm^2. Therefore, its role in the process of multiple ionization has been unclarified up to now.

The present paper aims at investigating multiple ionization in terms of the many-body theory of the tunneling effect in the fields with intensity of up to 10^{19} W/cm^2. The laser radiation is assumed to be linearly polarized, since, as mentioned above, impact ionization by rescattered photoelectron is suppressed due to the Lorentz force effect.

As compared to Refs. [17,18], the present paper contains the estimation of one more many-body effect: (iii) the ionic core relaxation with respect to the magnetic quantum numbers of electrons m. This effect has been considered both theoretically [24] and experimentally [25].

The next section presents the general equations describing the rate of collective ITE. In Sec. III the mechanism of the core relaxation with respect to the magnetic quantum numbers is under consideration; the estimation of the relaxation rate is presented. Section IV contains the kinetic equations for describing multiple ionization with the many-body effects taken into account. The results of computations of the probability of the Rb^{10+} and Rb^{11+} ion formations in various multiplet states are presented in Sec. V both for spatially homogeneous laser beam and for the beam with Gaussian distribution of intensity. In the present paper the atomic units ($\hbar = m_e = e = 1$) are used, except for specified cases.

II. RATE OF COLLECTIVE INELASTIC TUNNELING

The quantum-defect (QD) approximation, well known in the atomic and molecular physics [26], underlies the single-body ADK theory of tunneling effect. The applicability of the QD theory to the ground and low-lying excited states of atoms is substantiated in Ref. [27]. The rate of collective tunneling of several equivalent electrons was obtained in Ref. [19]. One more many-body effect was taken into account by the same author in Ref. [20]. This is the core excitation in the process of ITE. This ITE was proposed in Ref. [20] in terms of the approximation by Carlson [28], who considered the single-photon two-electron ionization of helium. When a He atom collides with a high-energy photon, the ionization time of one of the electrons is very short. The second electron may either remain in a bound state of the He^+ ion or be ionized due to the nonorthogonality of the single-electron states in a self-consistent field of the neutral He atom and the He^+ ion. Such mechanism of the He^{2+} formation reminds us of the well-known shake-up approximation [29], but formally differs from it, since the energy required for the ionization of the second (slow) electron is taken into account in the computation of the ionization rate of the first (fast) electron. Similar approximation has been used at the computation of the ITE [20]. Since the change in the self-consistent field in an outer shell is not taken into account, the excited states of a residual ion represent other components of the fine structure of the same multiplet, to which the ground state of a residual ion pertains. The agreement between theory [17] and experiment [23] demonstrates that such approximation is quite satisfactory for the problem under consideration.

Both many-body effects (collective and inelastic tunneling) can be described by a single formula, presented in Ref. [17] for the circularly polarized radiation. As far as linearly polarized radiation is concerned, the rate of inelastic collective tunneling of N equivalent electrons from the outer shell of a neutral atom or a positive ion is given by the following equation [30]:

$$W_{\kappa l\{m\}}^{(N,\mathrm{lin})} = \sqrt{\frac{6}{\pi}} \frac{M!\left(l+\frac{1}{2}\right)^N}{2^M N^{M+1}} \times C_{\kappa l}^{2N} Q^2 \kappa^{3N-1} \left(\frac{2F_a}{F}\right)^{2[(Z/\kappa)-1]N-M+(1/2)} \times \exp\left(-\frac{2NF_a}{3F}\right) \prod_{j=1}^{N} \frac{(l+m_j)!}{m_j!^2 (l-m_j)!}. \tag{1}$$

Here, the index $\{m\}$ stands for the set of magnetic quantum numbers of the emitted electrons $(m_1, m_2, \ldots, m_N)$, so that

$$M = \sum_{j=1}^{N} m_j,$$

l is the orbital quantum number of the electrons,

$$\kappa = \sqrt{\frac{2E^{(N)}}{N}}, \quad E^{(N)} = \sum_{j=1}^{N} E_j, \quad E_j = E_j^{(0)} - \Delta_j,$$

$E_j^{(0)}$ is the jth ionization potential of a parental atom (or an ion); Δ_j is the energy of a core excitation; $F_a = \kappa^3$ is the typical strength of the atomic field; F is the amplitude of the electric field strength of a laser wave; Z is the charge of the residual ion; and Q is the overlap integral. The overlap integrals have been calculated for p electrons in Ref. [17]; calculations for d electrons are given in Appendix B.

The constant $C_{\kappa l}$ in Eq. (1) is specified by the asymptotic behavior of the single-electron wave function of a free atom (or an ion) at $r \gg 1$,

$$\psi(\boldsymbol{r}) \approx C_{\kappa l} \kappa^{3/2} (\kappa r)^{N[(Z/\kappa)-1]} e^{-\kappa r} Y_{lm}(\hat{\boldsymbol{r}}).$$

The most accurate method of calculating $C_{\kappa l}$ is the direct numerical integration of the Hartree-Fock equations for a free atom. In order to calculate $C_{\kappa l}$ in the QD approximation, it is necessary to know the Rydberg spectrum of an atom (or an ion) for the whole series considered [31]. There is no similar information for the MCIs with the outer d shells [32]. Therefore, the same expressions as in Refs. [12–14] are used in the present paper,

$$C_{\kappa l} = \frac{(2/\nu)^\nu}{\sqrt{2\pi\nu}}, \tag{2}$$

where $\nu = Z/\kappa$. The accuracy of these expressions can be judged by the results presented in Ref. [31].

The small value of the squared N-body Keldysh parameter.

$$\gamma^2 = \frac{\omega^2}{F^2} \frac{2E^{(N)}}{N} \ll 1, \tag{3}$$

where ω is the field frequency, and the small value of the external field strength as compared to the atomic field

$$F \ll F_a, \tag{4}$$

are the conditions of the validity of Eq. (1).

Condition (3) provides the tunneling regime of ionization. The rate of tunneling is independent on the field frequency. Condition (4) allows one to neglect the influence of the light field on the bound electron when deriving Eq. (1). Note that for the highly excited (Rydberg) states with large value of ν, condition (4) can be replaced with more rigorous one due to turning on barrier-suppression regime of ionization (for more details see Ref. [19]). The states of the parental and residual ions are included in Eq. (1) by means of the κ and Q parameters.

In Eq. (1) only the direct influence of the radiation on the ion is taken into account. Meanwhile, in case of linear polarization, the effects associated with rescattering can affect the MCI yield significantly. The tunneling ionization starts to compete with the impact ionization. The kneelike fractures appear on the curves, showing the dependence of the MCI yield on the laser intensity. However the increased radiation intensity results in an increase in the light magnetic component. The classical straight-line trajectory of the photoelectron transforms into an 8-like one resulting in the suppression of rescattering. For the Ti:sapphire laser (800 nm), the suppression of rescattering in the process of the Kr ionization has been observed at the intensity above 10^{16} W/cm^2 [5]. The intensities of that range are typical for the MCIs with the outer d shells. This circumstance allows one to consider theoretically the tunneling ionization of atoms by the linearly polarized radiation, neglecting the rescattering.

A single-body relativistic theory of tunneling ionization of an atomic ion proposed in Refs. [15,16] is suitable for the case when the binding energy of an electron in the ion is comparable to the rest energy of a free electron. The theory also takes into account the motion of the electron spin [16]. It is pointed out in these papers that the results of the relativistic and nonrelativistic theories coincide in fact if $Z<20$. The authors of Ref. [1] have also pointed to the nonrelativistic regime of tunneling in observing 16 charged ions. Thus, for the calculations performed in the present paper, relativistic effects are reduced only to the suppression of rescattering.

III. m RELAXATION

The role of the magnetic quantum number m in the MCI formation has been discussed in Ref. [24]. According to the data of that paper, the ionization of the electrons with zero projections of the total angular momenta onto the direction of the electric field of a linearly polarized radiation occurs at the initial stage of a laser pulse. The electrons having $|m| > 0$ ionize at higher intensity of radiation. As a result, specific angular distribution of photoelectrons takes place. However, the experimental data presented in Ref. [25] demonstrate that the fast m relaxation of the remaining electrons occurs in the process of sequential ionization.

The fast relaxation observed in Ref. [25] may be caused by electrostatic interaction between the electrons in the shell. This interaction leads to the formation of the total orbital momentum L of the shell under consideration (in LS coupling). To estimate its rate, we shall make use of the quantum uncertainty relation "energy time." Assuming the distance between the ionic level is ~ 1 eV (see Table I), we obtain the estimation of the m relaxation time $\tau_{\text{relax}} \simeq 6\times 10^{-16}$ s. This is significantly shorter than the value that the laser pulses used in the experiment in Ref. [25] [full width at half maximum (FWHM) 40 fs] as well as the pulses considered in the present research. Equation (1) actually contains the assumption of the fast m relaxation, since the presence of the overlap integrals in Eq. (1) implies that the time of formation of the LS states is much shorter than the inverse rate of the tunneling effect.

IV. KINETIC EQUATIONS

In the present paper the tunneling formation of MCIs is regarded as a multichannel cascading process. It includes

TABLE I. Ionization potentials of Rb^{X+} ions (the first terms) and their excitation energies (the next terms) according to the data published by the NIST [32].

Ion	Outer subshell		Energies (Ry)
Rb^{9+}	$3d^{10}$	$^1S_0$	20.32126
Rb^{10+}	$3d^9$	$^2D_{5/2}$	23.14618
		$^2D_{3/2}$	0.11263
Rb^{11+}	$3d^8$	$^3F_4$	26.88238
		$^3F_3$	0.10006
		$^3F_2$	0.14225
		$^1D_2$	0.31001
		$^3P_1$	0.42447
		$^3P_0$	0.43030
		$^3P_2$	0.43805
		$^1G_4$	0.52562
		$^1_0S_0$	1.15977
Rb^{12+}	d^7	$^4F_{9/2}$	30.70970
		$^4F_{7/2}$	0.08779
		$^4F_{5/2}$	0.13906
		$^4F_{3/2}$	0.17050
		$^4P_{3/2}$	0.36396
		$^4P_{5/2}$	0.39124
		$^2G_{9/2}$	0.40867
		$^2G_{7/2}$	0.49097
		$^2H_{11/2}$	0.55505
		$^2H_{9/2}$	0.64263
		$^2D_{5/2}$	0.58273
		$^2D_{3/2}$	0.72273
		$^2F_{5/2}$	0.87492
		$^2F_{7/2}$	0.919933
		$^2_1D_{3/2}$	1.35396
		$^2_1D_{5/2}$	1.39998

both single-electron and collective tunneling cascading transitions that can be accompanied by excitation of an ionic core. It is important that the number of cascading channels grows dramatically with the increase in the ionization multiplicity. Besides, the emitted electrons may have various projections of the orbital momentum m_q, leading to further branching of the cascading process and, consequently, to the increase in the number of ionization channels.

Multiple ionization of neutral atoms in the tunneling regime by a laser pulse is described successfully by the set of kinetic equations for the populations of various ionic states C_f [17],

$$\frac{dC_f}{dt} = \sum_{f'=0}^{f-1} W_{f\to f'} C_{f'} - \sum_{f'=f+1}^{f_{\text{tot}}} W_{f'\to f} C_f,$$

$$f = 0, 1, \ldots, f_{\text{tot}}, \tag{5}$$

$$C_0(-\infty) = 1, \quad C_1(-\infty) = \cdots = C_{f_{\rm tot}}(-\infty) = 0. \quad (6)$$

Indices f and f' in Eqs. (5) enumerate the ionic states. $W_{f'\to f}$ is the rate of tunneling transition from state $|f'\rangle$ to state $|f\rangle$, obtained from Eq. (1) by means of the replacement of the monochromatic field F with the pulse envelope $F(t)$.

Hereinafter we shall be interested in the ionization of the d shell at the laser intensity above 10^{17} W/cm^2. The total ionization of the outer shells of the neutral atoms occurs in the intensity range between 10^{14} and 10^{16} W/cm^2 [17,18]. Therefore, in front of the pulse all the atoms can be regarded to be ionized up to the term $d^{10}(^1S_0)$. Thus, the states $|d^k(vSL)JM_J\rangle$ (see Appendix A) correspond to the indices f and f'. In particular, f_0 defines the state $|d^{10}(^1S_0)00\rangle$ here. The quantity C_f should be regarded as the ratio between the ionic concentration n_f in the state $|f\rangle$ and the concentration of neutral atoms $n_{\rm tot}$ in a gaseous target (or $n_0 = n_{\rm tot}$ in the pulse front),

$$C_f(t) = n_f(t)/n_0(-\infty), \quad \sum_{f=0}^{f_{\rm tot}} n_f(t) = n_0(-\infty).$$

Initial conditions (6) are formulated for a point of time preceding the approach of the pulse front. Therefore, there is a formal presence of $-\infty$ in the arguments of C_f. The result of integrating the kinetic equations is a set of values $C_f(+\infty)$ corresponding to the concentrations in each ionic state after the laser-pulse completion.

V. RESULTS AND DISCUSSION

This section presents the results of integration kinetic Eqs. (5) describing the process of the MCI formation by a laser pulse with the Gaussian envelope $F(t) = F\exp[-\ln(2)t^2/T^2]$, where F is the peak strength of the electric field and T is the FWHM. In this case, it is sufficient to replace the argument $-\infty$ with $-2T$ in initial conditions (6) and to take $+2T$ as the upper limit of integration. The output parameters $C_f(+2T)$ are the functions of the maximum intensity in the pulse.

At present, there are sufficiently complete data on the spectra of the ions with the outer d shell only for $Rb^{9+}[d^{10}], \ldots, Rb^{12+}[d^7]$ (see Table I). Because of this, it is impossible to compare with the experimental data [2,4,25] on the ionization of the d shell of krypton since Kr and Rb ions with the same configurations have different charges.

In the present paper the yield of $Rb^{10+}, \ldots, Rb^{12+}$ ions is calculated as a function of the peak intensity I of a linearly polarized laser pulse with FWHM of 40 and 5 fs. Single-, two-, and three-electron collective transitions between all states, indicated in Table I are included in Eqs. (5). Only those excited states are taken into account, in which the principal quantum numbers do not change. Otherwise, the excitation energies increase by 1 or 2 orders, becoming comparable with the ionization potentials and leading to the exponential reduction in corresponding rates of tunneling. There are no data concerning the energies for the excited configuration of Rb^{12+}: ${}^2_3P_{1/2}$, ${}^2_3P_{3/2}$, and ${}^4_3P_{1/2}$. For the listed terms the assumed values of the energy of 1.17, 1.17, and 0.33 Ry were used, respectively. Twofold changes in these values do not affect appreciably the calculated yield of Rb^{10+} and Rb^{11+} ions. The limitation of the ionization multiplicity to 12 is caused by the lack of spectroscopic data. The authors do not present the results for the Rb^{12+} ions, as far as the correct account of the further ionization (Rb^{13+}) is not obviously possible.

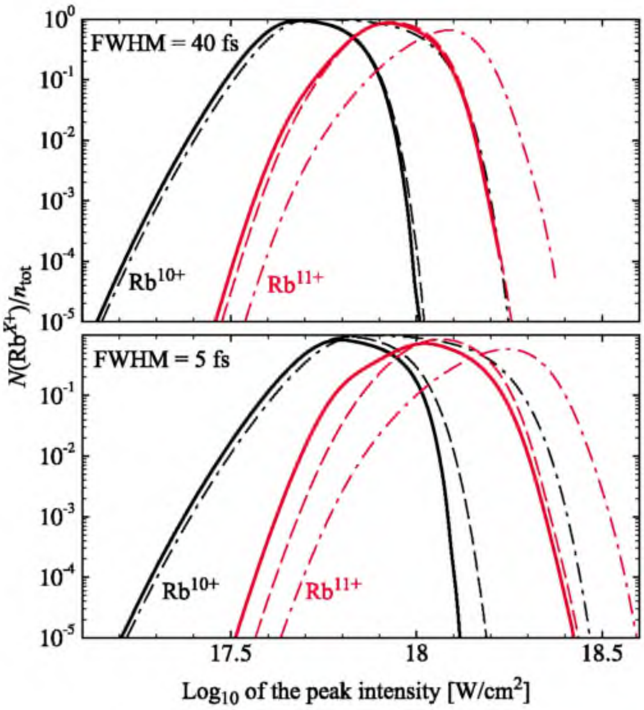

FIG. 1. (Color online) The total populations of the charged states of Rb^{10+} and Rb^{11+} in a gaseous target as functions of the peak intensity of a linearly polarized laser pulse I. Solid lines: $2e$ ITE. Dashed lines: $1e$ ITE. Dashed-dotted lines: ADK.

A. Ionic populations

Let us introduce the concentration of A^{X+} ions with the given multiplicity X in all the states of the d shell $|f_1(X)\rangle$, $|f_2(X)\rangle, \ldots, |f_{\max}(X)\rangle$,

$$n(A^{X+}) = \sum_{f=f_1(X)}^{f_{\max}(X)} n_f. \quad (7)$$

By analogy with Eq. (7), the ionic concentration with the given term $n[A^{X+}(vSLJ)]$ can be introduced. In all cases the summation over all values of the angular-momentum projections is implied in Eq. (7). In the present paper the values of $n(A^{X+})$ are calculated as functions of the peak intensity in the pulse after its completion. The obtained results are valid for a spatially homogeneous laser beam with an infinitely large focus diameter.

Figure 1 presents results of the calculation of $n(Rb^{10+})$ and $n(Rb^{11+})$ quantities as functions of the peak intensity I in a linearly polarized laser pulse. The results are divided into three groups. The first group corresponds to the only account of the sequential single-electron transitions between the ground states of the MCIs (the ADK model). In this case, 20 states of MCIs are involved in kinetic Eqs. (5). The number of possible ionization channels runs up to 210. The second group corresponds to all possible sequential single-electron transitions, including the ITE. The third group additionally includes collective two-electron tunneling transitions. In these cases, 173 states of MCIs are involved in kinetic Eqs. (5). The number of possible ionization channels exceeds 50 000. Three-electron collective tunneling effect in the $Rb^{9+} \to Rb^{12+}$ channels does not influence on the result noticeably and, therefore, is not presented in the figures.

As in the case with the p shell [17,18], taking into account the core excitation does not actually affect the process of ionization of the first electron in the region of the rise of the Rb^{10+} ion population. Similar to the results of Refs. [17,18], the difference from the ADK model by 1 or 2 orders is revealed only in the ionization of the second electron in the d shell (Rb^{11+}). That is the consequence of the dramatic increase in the number of ionization channels. As contrasted with the results of Refs. [17,18], in the case of the d shell the two-electron ITE becomes noticeable. It becomes apparent in the process of Rb^{11+} ion formation. If, at the FWHM of 40 fs, the contribution of the two-electron process exceeds that of one electron by 1.5 or 2 times, then in case with the FWHM of 5 fs and, respectively, higher intensity this difference may reach 1 order of magnitude. The difference between single- and two-electron ITEs for the Rb^{10+} ions becomes apparent only in the region of the population decrease. Note that the two-electron ITE was extremely negligible in the populations of the charge states of $Ar^{1+}, \ldots, Ar^{5+}$ and $Kr^{1+}, \ldots, Kr^{5+}$ ions only far from the saturation points.

In Ref. [19] it was pointed out that the collective two-electron tunneling effect may be more probable than the sequential single-electron tunneling. This fact is caused by the structure of the exponential factors in Eq. (1). However, taking into account the saturation of the concentration of ions with lower multiplicity and pre-exponential factors in Eq. (1), it is impossible to conclude unambiguously about the collective tunneling without the detailed calculations.

In a real case the intensity in a laser beam is not spatially homogeneous. The procedure of the reduction in the experimental results to the spatially uniform distribution of intensity has been proposed in Ref. [33]. It is based on the method of intensity selective scanning in the beam [34]. By means of this procedure, the populations of the $Ar^{1+}, \ldots, Ar^{5+}$ ions were measured in Ref. [23] after the impact of a circularly polarized laser pulse with the FWHM of 50 fs and the central wavelength of 790 nm on the gas. The given experiment completely confirmed the many-body theory of the tunneling effect [17] used in this paper.

B. Close-to-real intensity distribution

Let us calculate the MCI yield in the case of the close-to-real distribution of the laser intensity corresponding to the focused beam with the diffraction taken into account. In most experiments (see, e.g., Ref. [25]) the ions are extracted from the total focal volume rather than from its separate elements [34]. Therefore, in addition to the population, it is necessary to obtain the absolute number of ions in the given states in the focal volume.

Let us consider a focused laser beam with the Gaussian distribution of the peak intensity over the cross-section diameter,

$$I(\boldsymbol{r}) = I_b(z)\exp\left[-\frac{2r^2}{r_b^2(z)}\right], \tag{8}$$

where

$$r_b(z) = r_0[1 + (z/z_0)^2]^{1/2},$$

$$I_b(z) = I[1 + (z/z_0)^2]^{-1},$$

where r_0 is the beam waist radius, I is the intensity of the beam axis in the waist (the absolute intensity), z_0 is the Rayleigh range given by $z_0 = \pi r_0^2/\lambda$, and λ is the laser wavelength. If we integrate $C_f(I(\boldsymbol{r}))$ over the beam volume, we will obtain the following integral spatially averaged ionic yield:

$$P_f(I) = n_{\text{tot}} \int C_f(I(\boldsymbol{r})) d^3r$$
$$= \frac{n_{\text{tot}}}{\lambda}(\pi r_0^2)^2 \int_0^{\infty} d\zeta (1 + \zeta^2) \int_0^{I/(1+\zeta^2)} C_f(I') \frac{dI'}{I'}, \tag{9}$$

where $\zeta = z/z_0$. Quantity (9) defines the absolute number of f-type ions within the focal volume. By analogy of Eq. (7), let us also introduce the spatially averaged yield $P(A^{X+})$ of A^{X+} ions in all the possible states.

The dependence of the $P(Rb^{10+})$ and $P(Rb^{11+})$ on the absolute intensity I at the FWHM of 40 and 5 fs is presented in Fig. 2. Here, spatial averaging maintains the noticeable distinction between the single- and two-electron ITEs. Such a distinction reduces with the decrease in the laser intensity. As well as in Refs. [17,18], here, we observe a significant difference (up to 2 orders) from the results obtained in the ADK model. A similar difference between the experimental data and the ADK model for the d shell of krypton is mentioned by the authors of Ref. [25].

C. Contribution of individual multiplets

In Sec. V A it was indicated that the proposed theory allows one to calculate the yield of the MCIs in the specific multiplet states. Figure 3 presents the results of the calculations for several multiplets at the FWHM of 5 fs. For the Rb^{10+} ions, the yield of all the possible multiplets ${}^2D_{3/2}$ and ${}^2D_{5/2}$ is shown. For the Rb^{11+} ions, the multiplets have been chosen giving the highest (${}^1G_4$) and the lowest (${}^3P_0$) yield. Similar to Figs. 1 and 2, Fig. 3 does not present the data, concerning the Rb^{12+} ions, the states of which were also taken into account in the solution of kinetic Eqs. (5).

Figure 3(a) presents the populations of the indicated multiplet states produced by the pulse with the infinite focal diameter (see Fig. 1). Figure 3(b) displays the more realistic case of the focused beam with the Gaussian distribution of intensity over diameter (8) (see also Fig. 2). The results of calculations are divided into two groups: (i) taking into account both single- and two-electron collective tunneling transitions; (ii) taking into account only single-electron tunneling

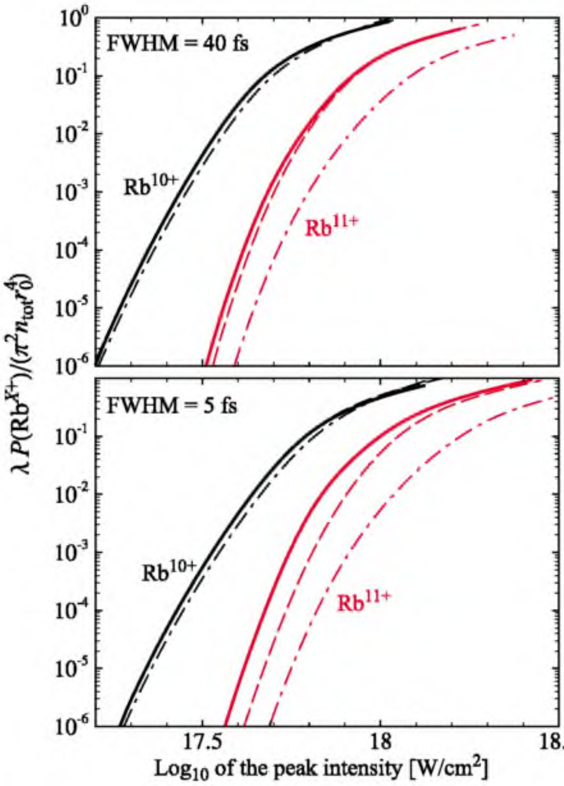

FIG. 2. (Color online) The yield of Rb^{10+} and Rb^{11+} ions averaged over focal volume in a gaseous target as a function of the absolute intensity of a linearly polarized laser pulse I. Designations are the same as in Fig. 1.

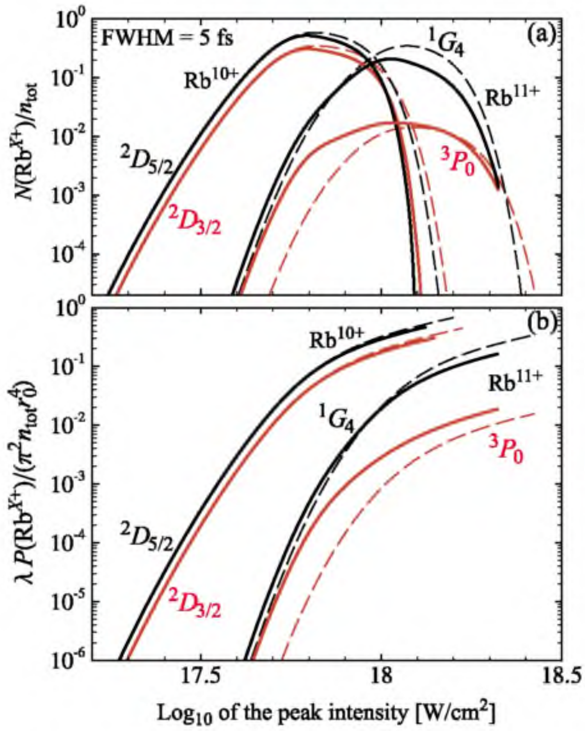

FIG. 3. (Color online) The population of Rb^{10+} and Rb^{11+} ion states (a) and their yield averaged over the focal volume (b) in a gaseous target as a function of the absolute intensity of a linearly polarized laser field I. Solid lines: $1e+2e$ ITE. Dashed lines: $1e$ ITE only.

transitions. The contribution of the three-electron collective tunneling transitions practically coincides with (i) and is not shown in Fig. 3.

With the intensity increase the populations of both multiplets of the Rb^{10+} ions, calculated with an account of the collective tunneling effect, appear to be lower than those obtained in the case of taking into account only the single-electron transitions. This fact is connected with the increase in ionization channel number.

The plots, corresponding to the rest Rb^{11+} multiplets, fill the space between the curves for ${}^1G_4$ and ${}^3P_0$ uniformly. The large number of the ionization channels makes it difficult to carry out the detailed analysis of the yield dependence of either of multiplets on the intensity. The values of kinetic coefficients $W_{f'\to f}$ are influenced not only by the binding energy of electrons but also by the overlap integrals and the single-electron quantum numbers.

VI. SUMMARY

The results of the calculations, presented in the paper and also in Refs. [17,18], confirmed by the experimental results [22,23], show that the basic mechanism, defining the difference between single-body and many-body models of MCI formation by the laser field, is the ITE, essential for all the realistic intensities that lead to formation of the ions with the multiplicity of 2 and higher. The examples of the Rb^{10+} and Rb^{11+} ions show that the two-electron collective tunneling effect becomes essential, changing the total probability of the ion formation more than by an order, if the radiation intensity is higher than $10^{17.5}$ W/cm^2. We shall point out for comparison that the relativistic effects change the probability of the tunneling ionization by an order in H-like ions only at $Z > 40$ [15].

ACKNOWLEDGMENT

This research was supported by the Russian Foundation for Basic Research (Grant No. 08-02-00337).

APPENDIX A: *d* SHELL WAVE FUNCTIONS

Considering the interaction of the outer d electrons of the ion with the laser radiation at the ionization multiplicity up to 20, the LS coupling approximation is valid. The state of the d^k shell ($k \leq 10$) is specified by the set of the quantum numbers ($vSLJM_J$). Here, J and M_J stand for the total momentum of the shell and its projection, respectively (in this case the quantization axis is chosen in the direction of the polarization vector of the laser radiation; $\boldsymbol{J}=\boldsymbol{L}+\boldsymbol{S}$; $\boldsymbol{L}$ and $\boldsymbol{S}$ are the total orbital momentum and the spin, respectively); $v \leq k$ is the so-called seniority number of the electron configuration. It presents that the minimum quantity of the electrons for which the state with the specified quantum numbers S and L occurs for the first time. Due to the spherical symmetry of a free atom, the total energy of a shell does not depend on the magnetic quantum number M_J. Thus, the energy of any term of the d^k is completely specified by the set of quantum the numbers $(vSLJ)$.

Let $\boldsymbol{r}_q$ be the radius vector of the q's electron; $\xi_q=(\boldsymbol{r}_q\sigma_q)$ is the set of its spatial and spin coordinates; $\xi^{(k)}=(\xi_1,\ldots,\xi_k)$ is the set of coordinates in the k-electron configuration. The wave function of the d^k shell in the coordinate representation can be conveniently constructed with the defined values of the total spin projection M_S and total orbital momentum projection M_L,

$$\langle\xi^{(k)}|d^k(vSL)M_SM_L\rangle. \tag{A1}$$

In the single-body approximation, wave function (A1) can be expressed as a linear combination of d^{k-1} shell wave functions given by Eq. (A1),

$$\begin{aligned}\langle\xi^{(k)}|d^k(vSL)M_SM_L\rangle &= R(r_q)Y_{2m_k}(\hat{\boldsymbol{r}}_k)\chi_{\mu_q}(\sigma_q)\\ &\times\sum_{v',S',L'}C^{SM_S}_{S'M_{S'}1/2\mu_k}C^{LM_L}_{L'M_{L'}2m_k}\\ &\times\langle d^{k-1}(v'S'L')d|d^k(vSL)\rangle\\ &\times\langle\xi^{(k-1)}|d^{k-1}(v'S'L')M_{S'}M_{L'}\rangle.\end{aligned} \tag{A2}$$

Here, $R(r)$ is the radial-wave function; $\chi(\sigma)$ is the spin function; $\langle d^{k-1}(v'S'L')d|d^k(vSL)\rangle$ is the coefficient of fractional parentage (CFP). For $k=3,\ldots,5$, the coefficients were first tabulated in Ref. [35]. These data provide antisymmetry of the wave function with respect to the permutation of any pair (ξ_i,ξ_j). In the case of d^2 configuration, the CFPs are equal to unity if $L+S$ is even and to zero if $L+S$ is odd. If the d shell is filled in by a single electron, then the sum in Eq. (A2) reduces to unity. At a given k the wave functions in Eq. (A1) are orthogonal and normalized to unity,

$$\begin{aligned}&\langle d^k(v'S'L')M_{S'}M_{L'}|d^k(vSL)M_SM_L\rangle\\ &=\delta_{v'v}\delta_{S'S}\delta_{L'L}\delta_{M_{S'}M_S}\delta_{M_{L'}M_L}.\end{aligned} \tag{A3}$$

Below the permitted sets (vSL) are listed for various configurations of d^k in the spectroscopic notation (the seniority number is indicated in the lower-left position),

$$d^0:{}^1S,$$

$$d^1:{}^2D,$$

$$d^2:{}^1_0S,{}^3P,{}^1D,{}^3F,{}^1G,$$

$$d^3:{}^2P,{}^4P,{}^2_1D,{}^2D,{}^2F,{}^4F,{}^2G,{}^2H,$$

$$d^4:{}^1_0S,{}^1S,{}^3_2P,{}^3P,{}^1_2D,{}^1D,{}^3D,{}^5D,{}^1F,{}^3_2F,{}^3F,{}^1_2G,{}^1G,{}^3G,{}^3H,{}^1I,$$

$$d^5:{}^2S,{}^6S,{}^2_3P,{}^4_3P,{}^2_1D,{}^2_3D,{}^2D,{}^4D,{}^2_3F,{}^2F,{}^4_3F,{}^2_3G,{}^2G,{}^4G,{}^2_3H,{}^2I.$$

In the case when the d^k shell is filled more than half ($k=6,\ldots,10$), then the same (vSL) sets are permitted for the d^{10-k} configuration. In this case, the CFPs are calculated by the recurrent formula from Ref. [35],

$$\begin{aligned}\langle d^{k-1}(v'S'L')d|d^k(vSL)\rangle &= (-1)^{S+S'+L+L'-(5/2)}\\ &\times\left[\frac{11-k}{k}\frac{2S'+1}{2S+1}\frac{2L'+1}{2L+1}\right]^{1/2}\\ &\times\langle d^{10-k}(vSL)d|d^{11-k}(v'S'L')\rangle.\end{aligned}$$

The states $|d^k(vSL)JM_J\rangle$ are obtained from Eq. (A1) in accordance with the rule of the vector summation of angular momenta,

$$|d^k(vSL)JM_J\rangle=\sum_{M_S,M_L}|d^k(vSL)M_SM_L\rangle C^{JM_J}_{LM_LSM_S}. \tag{A4}$$

APPENDIX B: OVERLAP INTEGRALS

The many-body structure of the ion wave functions comes into the rates of the tunneling ionization through the squared overlap integrals Q. However, it seems more convenient to obtain the overlap integral $\widetilde{Q}$ for the tunneling N-electron transition from the initial state with k electrons $|d^k(v_kS_kL_k)M_{S_k}M_{L_k}\rangle$ to the final state with $k-N$ electrons $|d^{k-N}(v_{k-N}S_{k-N}L_{k-N})M_{S_{k-N}}M_{L_{k-N}}\rangle$ in representation (A1). Let us neglect the variation in the wave functions of the completely filled internal shells [36].

For arbitrary k and N, expression (A2) can be presented in the form of expansion over the basis functions $\langle\xi^{(k-N)}|d^{k-N}(v_{k-N}S_{k-N}L_{k-N})M_{S_{k-N}}M_{L_{k-N}}\rangle$ by means of sequential N-fold performing,

$$\begin{aligned}&\langle\xi^{(k)}|d^k(v_kS_kL_k)M_{S_k}M_{L_k}\rangle\\ &=\sum_{[(vSL)M_SM_L]_{k-N}}\sum_{\text{all }m\mu}\widetilde{Q}^{(m_{k-N+1}\mu_{k-N+1},\ldots,m_k\mu_k)}_{\{kN;[(vSL)M_SM_L]_{k-N},[(vSL)M_SM_L]_k\}}\\ &\times\prod_{q=k-N+1}^{k}R(r_q)Y_{2m_q}(\hat{\boldsymbol{r}}_q)\chi_{\mu_q}(\sigma_q)\\ &\times\langle\xi^{(k-N)}|d^{k-N}(v_{k-N}S_{k-N}L_{k-N})M_{S_{k-N}}M_{L_{k-N}}\rangle.\end{aligned}$$

Here, (m_q,μ_q) is the set the projections of the orbital and spin momenta of emitted electrons. We have introduced the notation

$$[\alpha\beta\ldots]_i\equiv(\alpha_i,\beta_i,\ldots).$$

The expansion coefficients $\widetilde{Q}$ will correspond to the overlap integrals. They are given by the relatively simple recurrent formula

$$\begin{aligned}&\widetilde{Q}^{(m_{k-N+1}\mu_{k-N+1},\ldots,m_k\mu_k)}_{\{kN;[(vSL)M_SM_L]_{k-N},[(vSL)M_SM_L]_k\}}\\ &=\sum_{[vSL]_{k-N+1}}\langle d^{k-N}([vSL]_{k-N})d|d^{k-N+1}([vSL]_{k-N+1})\rangle\\ &\times C^{L_{k-N+1}M_{L_{k-N+1}}}_{L_{k-N}M_{L_{k-N}}2m_{k-N+1}}C^{S_{k-N+1}M_{S_{k-N+1}}}_{S_{k-N}M_{S_{k-N}}1/2\mu_{k-N+1}}\\ &\times\widetilde{Q}^{(m_{k-N+2}\mu_{k-N+2},\ldots,m_k\mu_k)}_{\{kN-1;[(vSL)M_SM_L]_{k-N+1},[(vSL)M_SM_L]_k\}}.\end{aligned} \tag{B1}$$

Here, the following is assumed for $N=0$:

$$\widetilde{Q}_{\{k0;[(vSL)M_SM_L]_k,[(vSL)M_SM_L]_k\}} = 1.$$

The quantities in Eq. (B1) have the following properties.

(1) In accordance with the Pauli principle, they change the sign after the permutation of any pairs of indices $(m_q\mu_q)$, corresponding to the emitted electrons,

$$\widetilde{Q}_{\{\cdots\}}^{(\ldots,m_i\mu_i,\ldots,m_j\mu_j,\ldots)} = -\,\widetilde{Q}_{\{\cdots\}}^{(\ldots,m_j\mu_j,\ldots,m_i\mu_i,\ldots)}. \tag{B2}$$

(2) The orthogonality condition (A3) leads to satisfying the following summation rule:

$$\sum_{[(vSL)M_SM_L]_{k-N}} \sum_{\text{all } m\mu} [\widetilde{Q}_{\{kN;[(vSL)M_SM_L]_{k-N},[(vSL)M_SM_L]_k\}}^{(m_{k-N+1}\mu_{k-N+1},\ldots,m_k\mu_k)}]^2 = 1. \tag{B3}$$

The sets of quantities in Eq. (B1) may be tabulated by means of any computer algebra system. Properties (B2) and (B3) can be used for the verification of results.

The overlap integrals Q between the states $|d^k(vSL)JM_J\rangle$ are obtained from $\widetilde{Q}$ by means of Eq. (A4). Using the orthogonality condition of the Clebsch-Gordan coefficients, the following formula is obtained:

$$\begin{aligned}
&[Q_{\{kN;[(vSL)M_LJ]_{k-N},[(vSL)M_LJ]_k\}}^{(m_{k-N+1},\ldots,m_k)}]^2 \\
&\quad = \sum_{(M_SM_J)_{k-N}} \sum_{(M_SM_J)_k} \sum_{\text{all }\mu} [C_{L_kM_{L_k}S_kM_{S_k}}^{J_kM_{J_k}}]^2 [C_{L_{k-N}M_{L_{k-N}}S_{k-N}M_{S_{k-N}}}^{J_{k-N}M_{J_{k-N}}}]^2 \\
&\qquad \times [\widetilde{Q}_{\{kN;[(vSL)M_SM_L]_{k-N},[(vSL)M_SM_L]_k\}}^{(m_{k-N+1}\mu_{k-N+1},\ldots,m_k\mu_k)}]^2.
\end{aligned} \tag{B4}$$

Since the tunneling ionization rate does not depend on the spin projections, the summations with respect to the corresponding quantum numbers are performed in Eq. (B4).

[1] E. A. Chowdhury, C. P. J. Barty, and B. C. Walker, Phys. Rev. A **63**, 042712 (2001).

[2] M. Dammasch, M. Dörr, U. Eichmann, E. Lenz, and W. Sandner, Phys. Rev. A **64**, 061402(R) (2001).

[3] K. Yamakawa, Y. Akahane, Y. Fukuda, M. Aoyama, N. Inoue, and H. Ueda, Phys. Rev. A **68**, 065403 (2003).

[4] K. Yamakawa, Y. Akahane, Y. Fukuda, M. Aoyama, N. Inoue, H. Ueda, and T. Utsumi, Phys. Rev. Lett. **92**, 123001 (2004).

[5] E. Gubbini, U. Eichmann, M. P. Kalashnikov, and W. Sandner, J. Phys. B **38**, L87 (2005).

[6] S. Palaniyappan, A. DiChiara, I. Ghebregziabher, E. L. Huskins, A. Falkowski, D. Pajerowski, and B. C. Walker, J. Phys. B **39**, S357 (2006).

[7] E. Gubbini, U. Eichmann, M. Kalashnikov, and W. Sandner, J. Phys. B **39**, S381 (2006).

[8] A. D. DiChiara, I. Ghebregziabher, R. Sauer, J. Waesche, S. Palaniyappan, B. L. Wen, and B. C. Walker, Phys. Rev. Lett. **101**, 173002 (2008).

[9] L. D. Landau and E. M. Lifshitz, *The Classical Theory of Fields* (Pergamon, Oxford, 1991).

[10] P. B. Corkum, Phys. Rev. Lett. **71**, 1994 (1993).

[11] L. V. Keldysh, Sov. Phys. JETP **20**, 1307 (1964).

[12] B. M. Smirnov and M. I. Chibisov, Sov. Phys. JETP **22**, 585 (1965).

[13] A. M. Perelomov, V. S. Popov, and M. V. Terent'ev, Sov. Phys. JETP **23**, 924 (1966).

[14] M. V. Ammosov, N. B. Deloné, and V. P. Kraĭnov, Sov. Phys. JETP **64**, 2008 (1986).

[15] N. Milosevic, V. P. Krainov, and T. Brabec, Phys. Rev. Lett. **89**, 193001 (2002).

[16] V. S. Popov, B. M. Karnakov, V. D. Mur, and S. G. Pozdnyakov, JETP **102**, 760 (2006).

[17] A. S. Kornev, E. B. Tulenko, and B. A. Zon, Phys. Rev. A **68**, 043414 (2003).

[18] A. S. Kornev, E. B. Tulenko, and B. A. Zon, Phys. Rev. A **69**, 065401 (2004).

[19] B. A. Zon, JETP **89**, 219 (1999).

[20] B. A. Zon, JETP **91**, 899 (2000).

[21] U. Eichmann, M. Dörr, M. Maeda, W. Becker, and W. Sandner, Phys. Rev. Lett. **84**, 3550 (2000).

[22] D. N. Fittinghoff, P. R. Bolton, B. Chang, and K. C. Kulander, Phys. Rev. A **49**, 2174 (1994).

[23] W. A. Bryan, S. L. Stebbings, J. McKenna, E. M. L. English, M. Suresh, J. Wood, B. Srigengan, I. C. E. Turcu, J. M. Smith, E. J. Divall, C. J. Hooker, A. J. Langley, J. L. Collier, I. D. Williams, and W. R. Newell, Nat. Phys. **2**, 379 (2006).

[24] R. Taieb, V. Véniard, and A. Maquet, Phys. Rev. Lett. **87**, 053002 (2001).

[25] E. Gubbini, U. Eichmann, M. P. Kalashnikov, and W. Sandner, Phys. Rev. Lett. **94**, 053602 (2005).

[26] Ch. Jungen, *Molecular Applications of Quantum Defect Theory* (Institute of Physics, Bristol, 1996).

[27] V. E. Chernov, D. L. Dorofeev, I. Yu. Kretinin, and B. A. Zon, Phys. Rev. A **71**, 022505 (2005).

[28] T. A. Carlson, Phys. Rev. **156**, 142 (1967).

[29] L. D. Landau and E. M. Lifshitz, *Quantum Mechanics: Non-Relativistic Theory* (Pergamon, Oxford, 1991).

[30] In Eq. (1) all introduced misprints from Ref. [17] have been removed.

[31] A. S. Kornev, I. Yu. Kretinin, and B. A. Zon, Laser Phys. **19**, 231 (2009).

[32] Yu. Ralchenko, A. E. Kramida, J. Reader, and NIST ASD Team, *NIST Atomic Spectra Database (Version 3.1.5)* (National Institute of Standards and Technology, Gaithersburg, MD, 2008); http://physics.nist.gov/asd3

[33] W. A. Bryan, S. L. Stebbings, E. M. L. English, T. R. J. Goodworth, W. R. Newell, J. McKenna, M. Suresh, B. Srigengan, I. D. Williams, I. C. E. Turcu, J. M. Smith, E. J. Divall, C. J. Hooker, and A. J. Langley, Phys. Rev. A **73**, 013407 (2006).

[34] M. A. Walker, P. Hansch, and L. D. Van Woerkom, Phys. Rev. A **57**, R701 (1998).

[35] G. Racah, Phys. Rev. **63**, 367 (1943).

[36] This approximation is accepted further everywhere. It means that the internal shells are considered as "frozen."